First publ. in: Journal of Biological Chemistry 281 (2006), 16, pp. 10976-10982

Crystal Structure of the Sugar Binding Domain of the Archaeal Transcriptional Regulator TrmB*

Received for publication, November 30, 2005, and in revised form, February 9, 2006 Published, JBC Papers in Press, February 10, 2006, DOI 10.1074/jbc.M512809200

Michael Krug, Sung-Jae Lee, Kay Diederichs, Winfried Boos, and Wolfram Welte[1]

From the Department of Biology, University of Konstanz, 78457 Konstanz, Germany

TrmB is an α-glucoside-sensing transcriptional regulator controlling two operons encoding maltose/trehalose and maltodextrin ABC transporters of *Pyrococcus furiosus*. The crystal structure of an N-terminal truncated derivative of TrmB (amino acids 2–109 deleted; $TrmB_{\Delta 2-109}$) was solved at 1.5 Å resolution. This protein has lost its DNA binding domain but has retained its sugar recognition site. The structure represents a novel sugar-binding fold. $TrmB_{\Delta 2-109}$ bound maltose, glucose, sucrose, and maltotriose, exhibiting K_d values of 6.8, 25, 34, and 160 μM, respectively. $TrmB_{\Delta 2-109}$ behaved as a monomer in dilute buffer solution in contrast to the full-length protein, which is a dimer. Co-crystallization with bound maltose identified a binding site involving seven amino acid residues: Ser^{229}, Asn^{305}, Gly^{320}, Met^{321}, Val^{324}, Ile^{325}, and Glu^{326}. Six of these residues interact with the nonreducing glucosyl residue of maltose. The nonreducing glucosyl residue is shared by all substrates bound to TrmB, suggesting it as a common recognition motif.

Gene expression in archaea (1–4) relies on a eukaryotic-like transcription machinery and eukaryotic-like promoter elements but bacterial-like regulatory transcription factors (4–8). Several archaeal transcription regulators have been reported (9). One type is homologous to the Lrp/AsnC family (10). Lrs14 and LysM have been identified in the hyperthermophilic crenarchaeoton *Sulfolobus solfataricus* (11, 12), LrpA in the hyperthermophilic euryarchaeoton *Pyrococcus furiosus* (10), and Ptr1 and Ptr2 in *Methanococcus jannaschii* (13). NrpR, a repressor of *nif* expression in *Methanococcus maripaludis* has been shown to recognize two tandem operators and to be released from binding by 2-oxoglutarate (14). Others are the metal-dependent regulator (MDR1) from *Archaeoglobus fulgidus* (15), a tryptophan-sensitive transcription regulator TrpY from *Methanothermobacter thermautotrophicus* (16), a heat shock gene regulator (Phr) from *P. furiosus* (17), and TrmB for the trehalose/maltose ABC transporter from *Thermococcus litoralis* and *P. furiosus* (18, 19).

TrmB is the transcriptional repressor for the gene cluster encoding the trehalose/maltose ABC transporter in hyperthermophilic archaea *T. litoralis* and *P. furiosus* (18). This gene cluster is identical in both species (20) and consists of the genes *malE*, *malF*, *malG*, *treT*, *trmB*, and *malK* (21–23). The DNA binding sites for TrmB overlap the BRE-TATA box of the *malE* operon. TrmB also binds to an inverted repeat sequence upstream of the BRE-TATA box and in front of *frk*, a gene divergently oriented to *malE* and encoding an ATP-dependent fructokinase (24). The transcriptional repression of the *malE* operon by TrmB in an *in vitro* transcription assay is overcome by the substrates of the trehalose/maltose ABC transporter (*i.e.* maltose and trehalose) (18). Recently, a second operon in *P. furiosus* encoding an ABC transporter for maltodextrins was identified (25). The gene cluster encoding this transporter of *P. furiosus* consists of *mdxE* encoding the substrate-binding protein (PF1938), *mdxF* and *mdxG* encoding the two transmembrane permeases (PF1937 and 1936), *pulA* encoding amylopullulanase (PF1935), and *mdxK* encoding the ATP-hydrolyzing protein of the transporter (PF1933). MdxE, carrying the substrate recognition site of the transporter, has been crystallized with bound maltotriose (26). Thus, the maltodextrin ABC transporter is distinct in its substrate specificity from the trehalose/maltose ABC transporter, which recognizes maltose and trehalose but not maltodextrins. Recently, we found that TrmB also controls the *mdxE* operon of *P. furiosus* as a transcriptional repressor and showed that repression is abolished by maltotriose and sucrose but not by maltose or trehalose (19). Therefore, TrmB appears to act as a bifunctional transcription regulator acting on two different promoters and being differentially controlled by binding to different sugars. We constructed a truncated form of TrmB in which the N-terminal DNA binding domain (amino acids 2–109) is deleted. In contrast to the full-length protein (which is dimeric) the truncated form behaved as a monomer during molecular sieve chromatography. Its binding affinity for the various substrates was increased, but its sigmoidal binding characteristic toward maltose could no longer be observed. Here, we report the crystal structure of the truncated form of TrmB. The structure contains bound maltose and represents a novel form of a sugar binding fold. Since the binding of the different sugars results in differential operator recognition, they will elicit differential conformational changes in the intact repressor protein.

EXPERIMENTAL PROCEDURES

Construction of Truncated TrmB Proteins—All truncated TrmB mutants were cloned into pCS19, resulting in C-terminal His tag versions. We used 5′ target sequence primers containing an NcoI site (CCATGG) and a 3′ end encompassing the sequence primer of TrmB containing the BamHI site. PCR products and vector plasmid were digested with NcoI and BamHI and were ligated by T4 ligase. The resulting plasmids containing the target inserts began with methionine as the first translated codon within the NcoI site. The constructed plasmids were called pSL189, pSL190, and pSL191 for Δ2–30, Δ2–59, and Δ2–109, respectively. We transformed the constructed plasmids into *Escherichia coli* SF120 competent cells and purified the three mutants truncated in the N-terminal DNA binding domain, Δ2–30, Δ2–59, and Δ2–109 TrmB, by Ni^{2+}-NTA[2] affinity chromatography.

Site-directed Mutation Analysis in the Sugar Binding Motif of TrmB—We prepared coupled primers (codon and noncodon strands of the same length) containing a target site mutation in the middle position (MWG Biotech). 100 ng of plasmid DNA encoding $TrmB_{\Delta 2-109}$ was

* The costs of publication of this article were defrayed in part by the payment of page charges. This article must therefore be hereby marked "*advertisement*" in accordance with 18 U.S.C. Section 1734 solely to indicate this fact.

The atomic coordinates and structure factors (code 2F5T) have been deposited in the Protein Data Bank, Research Collaboratory for Structural Bioinformatics, Rutgers University, New Brunswick, NJ (http://www.rcsb.org/).

[1] To whom correspondence should be addressed. Tel.: 49-7531-882206; Fax: 49-7531-883183; E-mail wolfram.welte@uni-konstanz.de.

[2] The abbreviation used is: NTA, nitrilotriacetic acid.

used as template DNA for PCR with 20 pmol of both primers, 0.2 mM dNTP mixture, and 1.5 units of Pwo polymerase. The PCR protocol was 94 °C for 30 min, 55 °C for 45 min, and a long extension phase at 72 °C for 12 min. 16 cycles were performed. PCR products were purified by the Qiagen extraction kit. The eluted DNA samples were directly digested by DpnI for selective degradation of methylated template DNA for 1 h at 37 °C. DNAs were directly transformed into the *E. coli* SF120 competent cells. The transformants were selected on ampicillin (100 μg/ml)-containing LB plates. The plasmid DNAs were prepared by a plasmid miniprep kit (Qiagen). All site-directed mutations were checked by sequencing analysis (GATC Biotech, Konstanz, Germany).

Protein Purification and Molecular Sieve Chromatography—For the expression of truncated TrmB and the site-directed mutation proteins derived from it, cells were grown in 1 liter of NZA medium (10 g of NZ-amine A, 5 g of yeast extract, 7.5 g of NaCl/liter) and 100 μg of ampicillin/ml at 30 °C. 0.2 mM isopropyl 1-thio-β-D-galactopyranoside was added after the culture had reached OD 0.7 at 578 nm. Cells were grown for an additional 5 h at 37 °C and harvested by centrifugation. The pellet was resuspended in 20 ml of Ni^{2+}-NTA affinity solution (buffer I; 50 mM sodium phosphate, 300 mM NaCl, pH 7.5), ruptured in a French pressure cell at 16,000 p.s.i., and centrifuged for 30 min at 17,300 $\times$ *g*. The supernatant was heated to 80 °C for 10 min. After centrifugation of the precipitated proteins, the supernatant was loaded onto a Ni^{2+}-NTA superflow column from Qiagen equilibrated with buffer I. The column was washed with 50 mM imidazole and eluted with 250 mM imidazole, both in the same buffer. Protein-containing fractions were pooled and dialyzed against 200 mM sodium phosphate buffer, pH 8.0. $TrmB_{\Delta 2-109}$ was extremely well induced by 0.2 mM isopropyl 1-thio-β-D-galactopyranoside and remained soluble during incubation at 80 °C, allowing for removal of *E. coli* proteins. The final concentration of pure $TrmB_{\Delta 2-109}$ was about 1.0 mg/ml. It was kept frozen at −70 °C.

For molecular sieve chromatography of $TrmB_{\Delta 2-109}$, we used Superdex 200 HR10/30 (Amersham Biosciences) with equilibration buffer, 50 mM HEPES, pH 7.5, 300 mM KCl, and 0.4 ml/min as the rate of elution. Despite the fact that wild type TrmB is retained by a Superdex column (19), the truncated protein was successfully separated by this type of material. The column was calibrated by molecular mass standard: chymotrypsinogen A, 25 kDa; ovalbumin, 43 kDa; bovine serum albumin, 67 kDa; and aldolase, 158 kDa (Amersham Biosciences). Native molecular weight was calculated by comparison with standard marker proteins.

Protein Purification Prior to Crystallization Experiments—Cells were grown as described above, but the cell pellet was resuspended in running buffer consisting of 50 mM Tris-HCl, pH 8.0, 200 mM NaCl, and 50 mM imidazole. Cells were ruptured twice in a French pressure cell at 11,000 p.s.i. and subsequently centrifuged for 30 min at 50,000 $\times$ *g*. The supernatant was incubated at 80 °C for 20 min, and after centrifuging for 60 min at 100,000 $\times$ *g*, the supernatant was loaded onto an Ni^{2+}-NTA superflow column from Qiagen equilibrated with running buffer. After it was loaded, the column was washed with running buffer and eluted with elution buffer (50 mM Tris, pH 8.0, 200 mM NaCl, 250 mM imidazole) using a three-step gradient. The protein eluted at the final step (100% elution buffer) and was afterward concentrated in elution buffer (preventing protein precipitation) using Vivaspin concentrators from Vivascience equipped with a 10-kDa cut-off membrane. Final protein concentration was 10 mg/ml, determined using the extinction coefficient at 280 nm calculated according to Gill and Hippel (27).

Protein Crystallization and Data Collection—Crystals of $TrmB_{\Delta 2-109}$ were obtained using the sitting drop vapor diffusion method. 2 μl of protein solution (10 mg/ml in 50 mM Tris-HCl, pH 8.0, 200 mM NaCl, 250 mM imidazole, 10 mM maltose) were mixed with 2 μl of reservoir solution containing 100 mM sodium acetate trihydrate, pH 4.6, and 8% (w/v) PEG 4000 and equilibrated against the reservoir solution at 18 °C. Trigonal crystals (space group $P3_221$) grew to a size of $\sim 50 \times 40 \times 50$ μm^3. Heavy atom derivatives were obtained by soaking the native crystals in reservoir solution containing in addition 1 mM platinum and 1 mM uranylacetate, respectively. Soaking time was 4 h for the platinum derivatives and 10 min for the uranylacetate derivatives. Diffraction data were collected under cryogenic conditions. The crystals were flash frozen in liquid nitrogen in buffer corresponding to the equilibrated crystallization drops plus 20% (v/v) glycerol as a cryoprotectant. All data sets were collected at the Swiss Light Source (SLS; beamline X06SA) provided with a MarCCD detector and were processed using XDS (28) and subsequently merged in XSCALE. More details of the data collection statistics are shown in Table 2.

Crystal Structure Determination and Refinement—The crystallographic phase problem was solved by multiple isomorphous replacement plus anomalous differences using one native data set, one platinum derivative data set, one uranylacetate derivative data set, and one native data set measured at a wavelength of 1.5 Å, allowing the search for the anomalous signal of the sulfur atoms inherent to the protein. The multiple isomorphous replacement plus anomalous differences experiment was done using the program suites SOLVE (29) and RESOLVE (30). One platinum site, one uranylacetate site, and four sulfur sites were found by SOLVE and used to determine initial phases. Subsequently, RESOLVE led to an interpretable electron density map and an initial model.

Model building and refinement was done using the CCP4 suite (31) and the graphical model building program COOT (32) for visual inspection and manual improvement of the model. Side chain atoms as well as other missing parts of the structure were added manually, followed by refinement cycles, including anisotropic B-factor refinement in REFMAC5 (33, 34). Model statistics are summarized in Table 3.

Sugar Binding and Inhibition Assay by TrmB—The binding tests were done by the ammonium sulfate precipitation method (35). A 100-μl aliquot of 50 mM HEPES, pH 7.5, 300 mM KCl containing 3.4 or 6.8 μM $TrmB_{\Delta 2-109}$ was incubated with 0.1 μCi of [^{14}C]maltose (0.65 μM) (Amersham Biosciences), [^{14}C]maltotriose (0.47 μM), [^{14}C]sucrose (0.4 or 0.8 μM) (Amersham Biosciences), or ^{14}C-glucose (8 μM) (PerkinElmer Life Sciences). [^{14}C]Maltotriose was synthesized from [^{14}C]maltose by the action of *E. coli* amylomaltase without loss of specific activity (36). Prior to their addition, the labeled sugars had been mixed with unlabeled sugars to reach a final concentration between 5 and 1,000 μM. Incubation was for 5 min at 70 °C. The assay was stopped with 2 ml of ice-cold saturated ammonium sulfate in binding buffer and kept on ice for 10 min. The suspension was then filtered through cellulose nitrate membrane filters (Schleicher & Schüll; pore size 0.45 μm) and washed with 1 ml of 95% saturated ammonium sulfate in binding buffer. Bound radioactivity was determined in a scintillation counter. Also, labeled sugar-binding inhibition assays with other sugars (maltose, maltotriose, sucrose, and glucose) were done in the same way with inhibiting sugars present between 25 and 500 μM, respectively.

RESULTS

Purification of Truncated TrmB—Mainly due to the tendency of TrmB to precipitate from solutions exceeding 1 mg/ml, attempts to crystallize the full-length TrmB protein have so far not been successful. Because of our experience that eubacterial repressor fragments can be crystallized after deletion of the N-terminal DNA binding domain, we constructed several N-terminal truncated TrmB variants as C-terminal

His tag versions and tested them for maltose-binding affinity. Of three constructs (Δ2–32, Δ2–59, and Δ2–109)[3] only one (Δ2–109) was not degraded, was highly soluble, and was expressed in large amounts after induction with 0.2 mM isopropyl 1-thio-β-D-galactopyranoside. $TrmB_{\Delta 2-109}$ was homogeneous on SDS-PAGE after Ni^{2+}-NTA affinity chromatography. From 1 liter of rich medium, 20 mg of pure $TrmB_{\Delta 2-109}$ was routinely obtained. The protein was stored frozen in 50 mM HEPES, pH 7.5, 300 mM KCl at a protein concentration of 1 mg/ml without loss of maltose binding activity.

Using molecular sieve chromatography (Superdex 200) in 50 mM HEPES, pH 7.5, 300 mM KCl at room temperature $TrmB_{\Delta 2-109}$ eluted with a peak corresponding to a species of 30 kDa (Fig. 1*A*), indicating that the protein was monomeric. However, the peak showed considerable trailing, which reflects interactions with the gel matrix.

Sugar Binding Activity of $TrmB_{\Delta 2-109}$—Full-length TrmB can bind maltose, trehalose, maltotriose, longer maltodextrins, sucrose, and glucose but not fructose, galactose, ribose, and lactose. $TrmB_{\Delta 2-109}$ showed the same binding specificity but increased binding affinity toward the same sugars compared with intact TrmB. This was particularly evident with maltose as substrate. The binding isotherm for all sugars, including maltose, was hyperbolic and exhibited a stoichiometry of about 1:1 (substrate/polypeptide). It showed the following K_d values: 6.8 μM for maltose, 25 μM for glucose, 34 μM for sucrose, and 160 μM for maltotriose (Fig. 2). Inhibition studies (Table 1) showed mutual competitiveness, indicating that all sugars were bound at the same site. We emphasize that binding of these sugars by full-length TrmB is sigmoidal only for maltose (18). Applying the criteria described previously (18), sigmoidality could not be detected in the binding kinetics of maltose in $TrmB_{\Delta 2-109}$.

Crystal Structure of $TrmB_{\Delta 2-109}$—The crystals were trigonal, $P3_221$, with unit cell axes of $a = b = 56.9$ Å, $c = 132.5$ Å, and contained one $TrmB_{\Delta 2-109}$ in the asymmetric unit. Experimental phases were obtained by isomorphous replacement and anomalous scattering (see "Experimental Procedures" and Tables 2 and 3). Fig. 3 shows the structure of $TrmB_{\Delta 2-109}$ in a *ribbon* representation.

$TrmB_{\Delta 2-109}$ consists of two domains, termed the N- and C-domains, formed by residues Ala^{110}–Gly^{246} and Lys^{249}–Ser^{342}, respectively. The two residues Asn^{247} and Pro^{248} may serve as a hinge. The N-domain

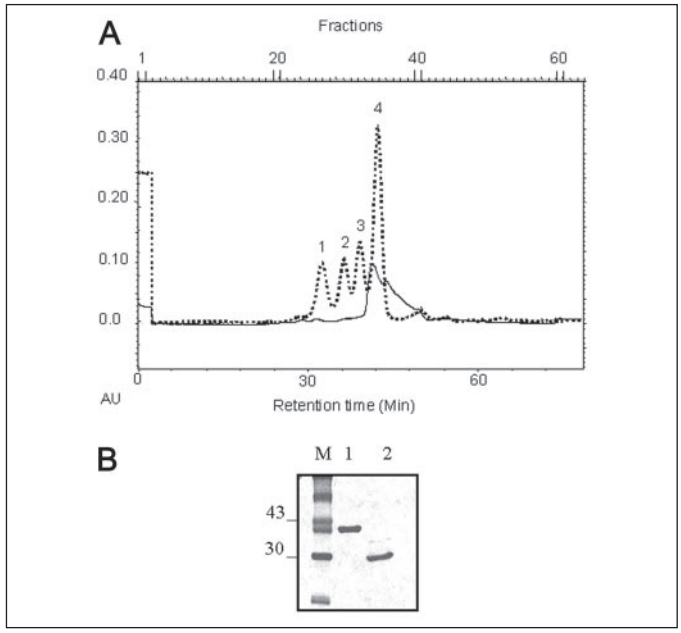

FIGURE 1. **Molecular sieve chromatography of $TrmB_{\Delta 2-109}$ and protein profile.** *A*, molecular sieve chromatography of $TrmB_{\Delta 2-109}$. The *dotted line* indicates molecular mass standards for aldolase (158 kDa) (*1*), bovine serum albumin (67 kDa) (*2*), ovalbumin (43 kDa) (*3*), and chymotrypsinogen A (25 kDa) (*4*). The apparent molecular weight was calculated by comparison with the standard marker proteins. These data show that $TrmB_{\Delta 2-109}$ is monomeric. *B*, SDS-PAGE of wild type TrmB (*lane 1*) and $TrmB_{\Delta 2-109}$ (*lane 2*).

[3] In the following, amino acids are numbered as in the full-length protein.

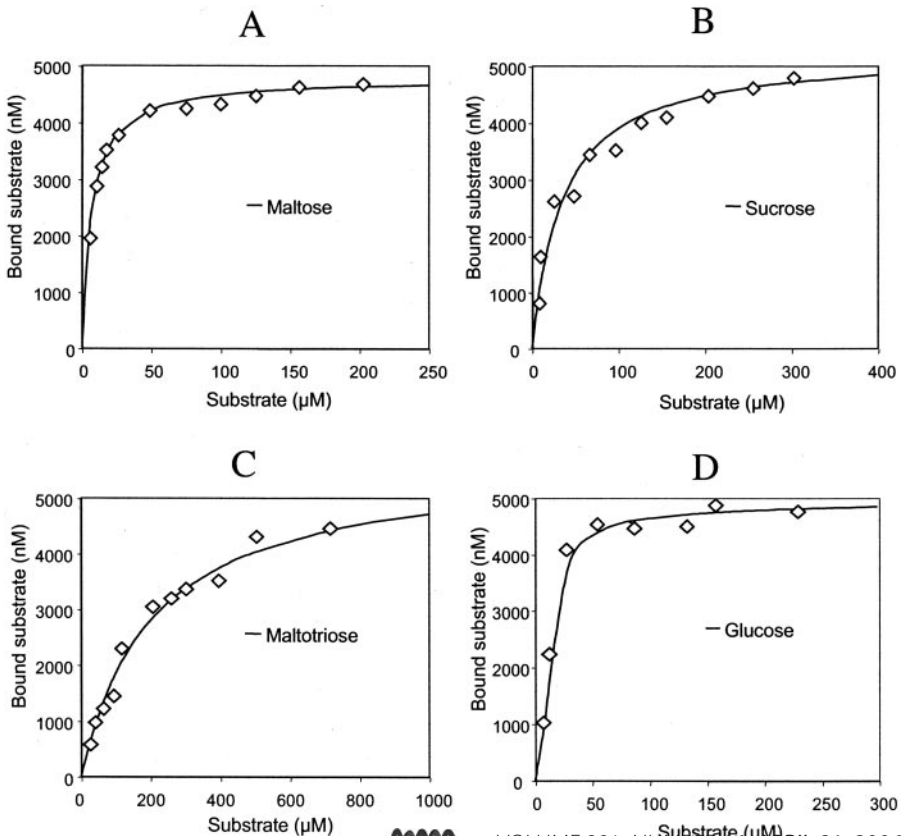

FIGURE 2. **Binding of maltose (*A*), sucrose (*B*), maltotriose (*C*), and glucose (*D*) by $TrmB_{\Delta 2-109}$.** The protein concentration was 6.8 μM for all sugar-binding assays. The K_d values estimated from the figures are 6.8, 25, 34, and 160 μM for maltose, glucose, sucrose, and maltotriose, respectively. Shown are the measured data points and the theoretical binding curves fitted according to a binding isotherm. The binding data for all sugars indicated a stoichiometry of 1:1 (substrate/polypeptide).

TABLE 1

Inhibition of binding of labeled substrate to $TrmB_{\Delta 2-109}$ by unlabeled sugars

^{14}C-Labeled sugars were present at 0.65, 0.47, 0.4, and 8 μM initial concentration for maltose, maltotriose, sucrose, and glucose, respectively. $TrmB_{\Delta 2-109}$ concentration was 3.4 μM. The values indicate the ratios of the amounts of bound labeled sugar in the presence and absence of competing unlabeled sugar in percent.

Bound labeled sugar	Maltose			Maltotriose			Sucrose			Glucose		
	25 μM	50 μM	100 μM	100 μM	250 μM	500 μM	50 μM	100 μM	250 μM	50 μM	100 μM	250 μM
	%	%	%	%	%	%	%	%	%	%	%	%
Maltose	29.0	12.0	9.5	86.5	58.2	48.4	31.1	18.5	9.4	22.3	9.5	3.9
Maltotriose	32.4	6.5	4.2	73.3	48.2	32.3	51.1	30.6	13.7	13.0	9.7	7.6
Sucrose	58.1	28.2	14.6	73.0	55.1	38.2	51.4	31.1	15.5	15.4	8.1	4.2
Glucose	5.0	3.2	3.0	100.	59.8	41.5	38.0	19.0	8.6	41.1	26.5	11.9

TABLE 2

Summary of data collection

	Native			Derivative		
	TrmB 1	TrmB 2	TrmB merged	TrmB-Pt	TrmB-UO_2Ac_2	TrmB-S
Wavelength (Å)	0.850	0.978		0.979	0.979	1.699
Cell (Å)	56.8, 56.8, 132.3	56.8, 56.8, 132.5	56.9, 56.9, 132.5	57.1, 57.1, 132.9	56.8, 56.8, 132.5	56.8, 56.8, 132.0
Resolution range (Å)	44–1.84 (1.94–1.83)	44–1.45 (1.54–1.45)	44–1.45 (1.54–1.45)	44–3.04 (3.23–3.04)	44–1.73 (1.84–1.73)	44–2.08 (2.21–2.08)
No. of unique reflections	41,989	43,837	44,046	9,229	49,611	27,781
Average multiplicity	3.75 (3.44)	10.47 (8.69)	13.99 (8.67)	4.04 (2.3)	5.29 (2.77)	11.16 (10.19)
$R_{mrgd\text{-}F}$ (%) (43)	5.1 (18.4)	3.4 (20.5)	3.3 (21.1)	7.3 (32.3)	12.2 (69.8)	4.7 (13.3)
Completeness (%)	99.4 (96.8)	98.0 (93.3)	88.0 (90.3)	99.1 (95.6)	99.5 (97.0)	97.8 (95.0)
I/σ_I	21.1 (7.3)	33.5 (7.3)	35.8 (7.9)	15.6 (3.4)	9.3 (1.8)	20.5 (9.5)

TABLE 3

Refinement statistics

Values given in brackets are for the highest resolution shell (1.49–1.45 Å).

Parameters	Values
Protein atoms	1,966
Ligand atoms	46
Solvent molecules	106
Resolution range	40–1.45 (1.49–1.45)
R-factor (%)	16.2 (17.2)
R-free (%)	19.5 (28.3)
Total number of reflections	41,765 (2,893)
Reflections in test set	2,224 (150)
Reflections in working set	39,541 (2,743)
B-factor of protein atoms (Å^2)	16.0
B-factor of all atoms (Å^2)	16.2
Root mean square deviation bonds (Å)	0.017
Root mean square deviation angles (degrees)	1.822
No. of residues with backbone conformational angles in most favored regions	191 (91.4%)
No. of residues with backbone conformational angles in additional allowed regions	17 (8.1%)
No. of residues with backbone conformational angles in generously allowed regions	1 (0.5%)
No. of residues with backbone conformational angles in disallowed regions	0 (0%)

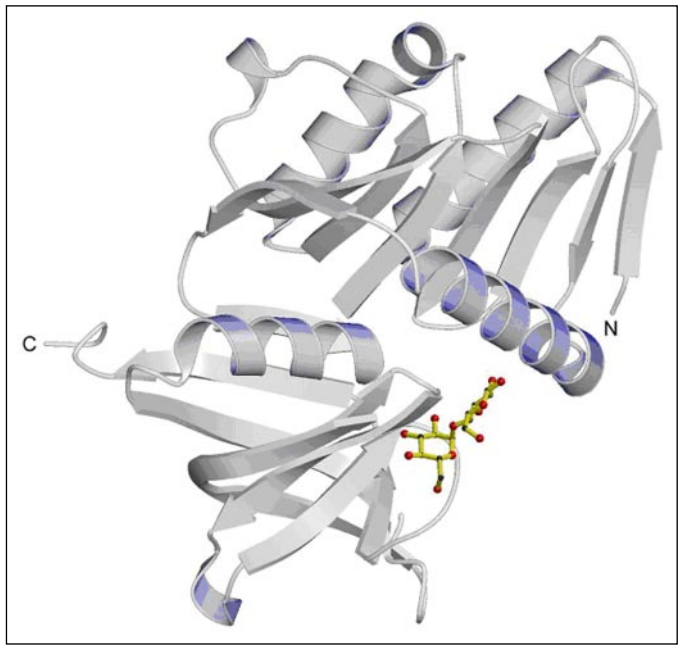

FIGURE 3. **Crystal structure of $TrmB_{\Delta 2-109}$.** The protein and the bound maltose are indicated as a *ribbon* and *ball and stick* representation, respectively. Maltose is bound with its nonreducing glucosyl residue toward the barrel domain. The N and C termini of the fragment are labeled.

forms an 8-stranded sheet flanked by two large helices on one side and one large helix crossing the β-sheet on the other side. Because the latter helix provides the only maltose-binding residues of the N-domain, we shall designate it as the "sugar binding helix" in the following. The C-domain forms a strand, a helix, and an irregular, flattened, seven-stranded β-barrel with its axis roughly parallel to the strands of the N-domain sheet. Most of the residues binding the nonreducing part of the maltose molecule are contributed by two neighboring loops of the C-domain barrel.

Maltose Binding in $TrmB_{\Delta 2-109}$—In the interstice between the two domains of $TrmB_{\Delta 2-109}$, electron density corresponding to maltose (α-D-glucosyl-1,4-α-D-glucose) was visible (Figs. 3 and 4). The nonreducing glucosyl residue of maltose forms hydrogen bonds with residues Asn^{305}, Gly^{320}, Met^{321}, Val^{324}, Ile^{325}, and Glu^{326}. All residues with the exception of Ser^{229} are in the C-domain and part of the β-sheet (Asn^{305}) as well as part of a loop region (Gly^{320}, Met^{321}, Val^{324}, Ile^{325}, and Glu^{326}). Ser^{229} in the sugar binding helix of the N-domain contributes the only hydrogen bond contacting the reducing glucosyl moiety of maltose.

Based on the observed mode of binding for maltose, it appears likely that all substrates are bound with their nonreducing α-glucosyl moiety to the same six amino acid residues of the C-domain. Obviously, the fixation of the common nonreducing glucosyl residue is the basis for the surprisingly large range of different substrates. Four of the maltose-interacting residues (Ser^{229}, Asn^{305}, Gly^{320}, and Glu^{326}) were changed by site-directed mutagenesis into alanine, and the purified proteins were analyzed for their binding affinity to maltose, maltotriose, sucrose, and glucose (Table 4). Whereas the mutant E326A lost all sugar binding affinity, mutants D305A and G320A showed reduced affinity. The mutant S229A showed reduced binding affinity only for maltose and maltotriose, whereas the affinity for sucrose and glucose remained the same as with the nonmutated $TrmB_{\Delta 2-109}$.

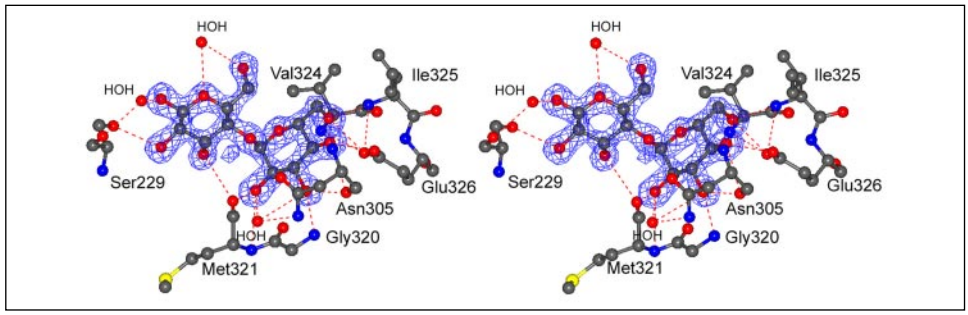

FIGURE 4. **Detail of $TrmB_{\Delta 2-109}$ around the maltose binding site in stereo.** The bound maltose and amino acid residues involved in binding are indicated as *ball and stick models*. The nonreducing glucosyl residue of maltose is oriented to the *right*. Residue numbers are indicated and correspond to the wild type protein. The 5σ level of the omit map of the bound maltose is shown as a *blue surface*.

TABLE 4

K_d values for sugar binding to $TrmB_{\Delta 2-109}$ and site-directed mutants

Shown are K_d values (μM) of site-directed mutants of $TrmB_{\Delta 2-109}$ at a protein concentration of 3.4 μM. —, no binding; ND, not determined.

Proteins	Maltose	Glucose	Sucrose	Maltotriose
			μM	
$TrmB_{\Delta 2-109}$	6.8	25	34	160
S229A	10	25	35	250
N305A	50	100	80	1,000
G320A	250	150	200	>2,000
E326A	—	—	—	—
N305A/G320A	—	ND	—	—
G320A/E326A	—	—	—	—

DISCUSSION

Comparison with Eubacterial Binding Proteins and Transcriptional Repressors—The maltose binding $TrmB_{\Delta 2-109}$ structure should be compared with the effector binding domains of the eubacterial *lac* repressor family members and eubacterial periplasmic binding proteins, which are thought to form a common structural class (37, 38). The periplasmic binding proteins are subdivided into groups with one, two, and three switches of the polypeptide between the two domains (39–41). These proteins undergo a large conformational change, moving the two domains against each other in such a way as to bury the substrate between them. The sugar binding pocket of $TrmB_{\Delta 2-109}$ does not resemble the canonical substrate binding pocket of eubacterial sugar-binding transcriptional regulators and periplasmic binding proteins. Although the N-domain and the barrel domain of $TrmB_{\Delta 2-109}$ participate in establishing the binding pocket, only the α-β N-domain resembles part of the eubacterial proteins, whereas the barrel domain has no counterpart among them.

In addition, whereas isopropyl 1-thio-β-D-galactopyranoside, maltose, maltotriose, maltotetraose, and trehalose are bound to the eubacterial proteins deeply in the cleft between both domains and with their axis oriented roughly along the cleft (41), the bound maltose in $TrmB_{\Delta 2-109}$ sticks to the surface-exposed edge of the cleft between the N- and the C-domain, oriented with its axis roughly perpendicular to the cleft (Fig. 5). The buried surface between the two domains is rich in phenylalanines and other hydrophobic residues, rendering a large movement of these domains in response to the sugar binding rather unlikely.

Alteration of the amino acid residues that are in contact with the bound maltose reveal the special role of Ser^{229}. The change to Ala only affects the binding of maltose and maltotriose but not the binding to sucrose and glucose (see Table 4). Ser^{229} is the only amino acid that contacts the reducing glucosyl residue of maltose. From these data, it is likely that sucrose interacts with the sugar binding helix on a site different from Ser^{229}. Possibly, it is the differential lateral movement of this helix in response to the binding of the different sugars that elicits the differential response in operator recognition. According to the structure of $TrmB_{\Delta 2-109}$, the DNA binding domain of the full-length TrmB is in proximity of the N-terminal end of the sugar binding helix, suggesting transduction of differential induced fit movements upon sugar binding via this helix.

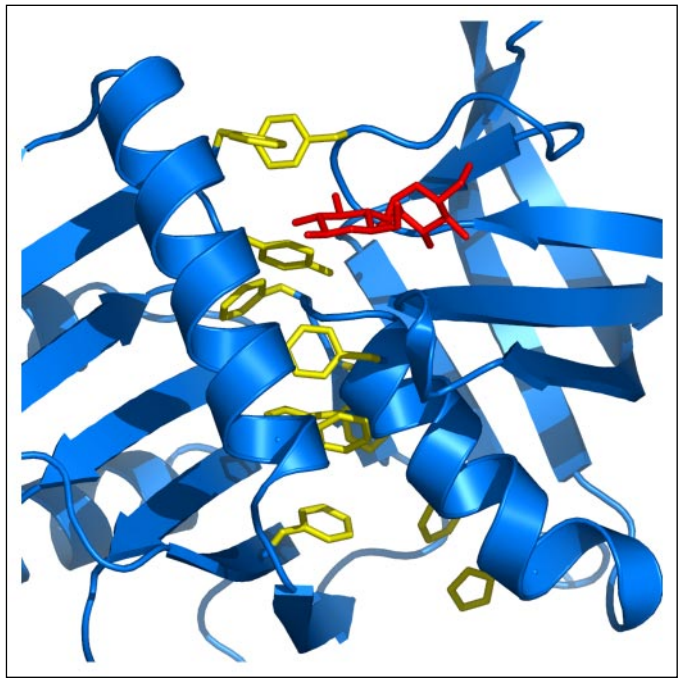

FIGURE 5. **Aromatic residues of the interdomain interface.** The protein, the bound maltose, and the aromatic residues are indicated as a *blue ribbon* and a *red* and *yellow bond representation*, respectively.

The $TrmB_{\Delta 2-109}$ Structure Represents a Novel Sugar-binding Structure—The result of a Dali search (42) with $TrmB_{\Delta 2-109}$ in the Protein Data Bank is summarized in Table 5. The three highest scores show only similarities between individual structural elements. Chain A of *E. coli* polyphosphate kinase (Protein Data Bank accession number 1xdo) yielded the highest score because of a similar barrel domain in both structures. Chain A of the calpain protease core was second because of the good superposition with the sugar binding helix of $TrmB_{\Delta 2-109}$. Chain A of a biotin ligase was third due to a poor superpo-

TABLE 5

Top hits of a Dali search with the structure of $TrmB_{\Delta 2-109}$

PDB, Protein Data Bank entry code; Z-score, strength of structural similarity in S.D. values above expected according to Ref. 42; RMSD, root mean square deviation of C_α coordinates of equivalenced residues in Å; LALI, total number of equivalenced residues; IDE, percentage of sequence identity over equivalenced residues.

PDB	Z-score	RMSD	LALI	IDE	Protein
				%	
1xdo	11.3	2.8	128	11	*E. coli* polyphosphate kinase
1kxr	5.0	3.0	76	11	Calcium-bound protease core of calpain I
1wnl	4.4	1.9	45	16	Biotin-(acetyl-CoA-carboxylase) ligase from *Pyrococcus horikoshii*

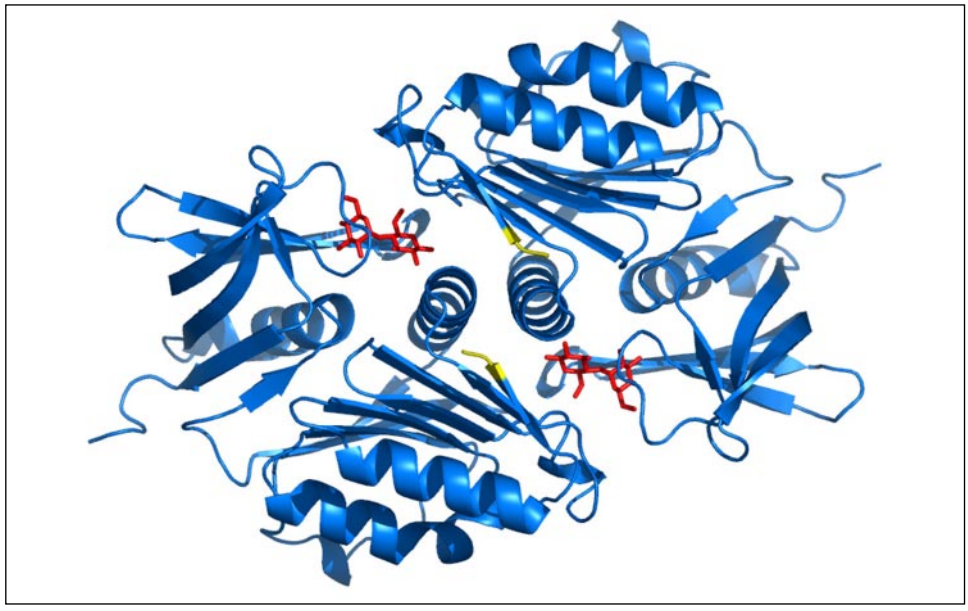

FIGURE 6. **Putative dimer structure of $TrmB_{\Delta 2-109}$.** A possible dimeric association of $TrmB_{\Delta 2-109}$ in a *ribbon representation* with the N terminus of the fragment in *yellow* and the two bound maltose molecules in a *red bond representation*.

sition with the N-domain of $TrmB_{\Delta 2-109}$. Thus, the structure and its mode of sugar binding are entirely novel.

The $TrmB_{\Delta 2-109}$ Structure in the Light of the in Vitro DNA Binding and Transcriptional Function of TrmB—TrmB binding to two intergenic DNA sites has previously been studied by electrophoretic mobility shift assay and footprinting analysis. One site is overlapping with and extending downstream of the BRE-TATA box of the *malE* operon (TM promoter) from *T. litoralis* and *P. furiosus* (18). A second site is nearly coincident with the transcriptional start point of the *mdxE* operon (MD promoter) in *P. furiosus*. The first site contains a palindromic motif 5′-TACTNNNAGTA-3′, whereas the second contains a distorted palindromic motif, 5′-TACTNNNATGG-3′ (19). From the perfect palindrome of the first site, one can conclude that TrmB binds there as a dimer with 2-fold symmetry relating one TrmB molecule and half of the palindrome to the remainder of the complex.

In the second site, most likely only the first half of the sequence (5′-TACTNNNA-3′) will contribute to the recognition of the TrmB dimer, resulting in a changed TrmB conformation. This prediction should hold despite the lack of knowledge about the structure of the N-terminal 109 residues of TrmB.

A possible quaternary structure of dimeric TrmB was selected from all crystallographic binary associates of $TrmB_{\Delta 2-109}$ as the one that buries the largest surface from solvent (2929 $Å^2$). In this association, the N termini are approximately parallel at a distance of only 12.7 Å (Fig. 6). Such a dimer of full-length TrmB would allow for a solvent-sequestered interface between the two DNA binding domains and would resemble several bacterial repressors that also bind to palindromic operators.

TrmB binding to DNA as detected by electrophoretic mobility shift assay as well as transcriptional repression *in vitro* has been found to be reduced upon the addition of specific sugar molecules (18, 19). Surprisingly, the inducibility by some of the sugars depended on the operons to which TrmB was bound, rendering TrmB a bifunctional transcriptional regulator: The TM operon was induced by maltose and trehalose but not by sucrose or maltodextrin, whereas the MD operon was induced by sucrose and maltodextrins but not by maltose or trehalose (19). In the absence of DNA, TrmB binds maltose, sucrose, glucose, maltotriose, and trehalose in decreasing order of affinity, and only maltose is bound in a cooperative manner. The structure of $TrmB_{\Delta 2-109}$ suggests explanations for these observations. When TrmB docks to the operator in front of the TM operon, due to the perfectly symmetric palindrome a complex of perfect 2-fold symmetry will result, exhibiting increased binding affinity for maltose and trehalose. However, when TrmB binds to the operator in front of the MD operon, due to the broken symmetry of the palindrome, allosteric effects will change the affinities of the sugar binding site so that sucrose and maltodextrins are preferentially bound. The delicate design of the sugar binding site across the cleft of the N- and C-domain, with the common nonreducing end bound to the C-domain and the other end pushing the sugar binding helix of the N-domain, is well suited for such allosteric changes.

REFERENCES

1. Thomm, M. (1996) *FEMS Microbial Rev.* **18,** 159–171
2. Kyrpides, N. C., and Ouzounis, C. A. (1999) *Proc. Natl. Acad. Sci. U. S. A.* **96,** 8545–8550
3. Soppa, J. (1999) *Mol. Microbiol.* **31,** 1295–1305
4. Geiduschek, E. P., and Ouhammouch, M. (2005) *Mol. Microbiol.* **56,** 1397–1407
5. Bell, S. D., and Jackson, S. P. (2001) *Curr. Opin. Microbiol.* **4,** 208–213
6. Reeve, J. N. (2003) *Mol. Microbiol.* **48,** 587–598
7. Ouhammouch, M. (2004) *Curr. Opin. Genet. Dev.* **14,** 133–138
8. Bell, S. D. (2005) *Trends Microbiol.* **13,** 262–265

9. Aravind, L., and Koonin, E. V. (1999) *Nucleic Acids Res.* **27,** 4658–4670
10. Brinkman, A. B., Dahlke, I., Tuininga, J. E., Lammers, T., Dumay, V., de Heus, E., Lebbink, J. H. G., Thomm, M., de Vos, W. M., and van der Oost, J. (2000) *J. Biol. Chem.* **275,** 38160–38169
11. Bell, S. D., and Jackson, S. P. (2000) *J. Biol. Chem.* **275,** 31624–31629
12. Brinkman, A. B., Bell, S. D., Lebbink, R. J., de Vos, W. M., and van der Oost, J. (2002) *J. Biol. Chem.* **277,** 29537–29549
13. Ouhammouch, M., Dewhurst, R. E., Hausner, W., Thomm, M., and Geiduschek, E. P. (2003) *Proc. Natl. Acad. Sci. U. S. A.* **100,** 5097–5102
14. Lie, T. J., Wood, G. E., and Leigh, J. A. (2005) *J. Biol. Chem.* **280,** 5236–5241
15. Bell, S.D., Cairns, S. S., Robson, R. L., and Jackson, S. P. (1999) *Mol. Cell* **4,** 971–982
16. Xie, Y., and Reeve, J. N. (2005) *J. Bacteriol.* **187,** 6419–6429
17. Vierke, G., Engelmann, A., Hebbeln, C., and Thomm, M. (2003) *J. Biol. Chem.* **278,** 18–26
18. Lee, S-J., Engelmann, A., Horlacher, R., Qu, Q., Vierke, G., Hebbeln, C., Thomm, M., and Boos, W. (2003) *J. Biol. Chem.* **278,** 983–990
19. Lee, S-J., Moulakakis, C., Koning, S. M., Hausner, W., Thomm, M., and Boos, W. (2005) *Mol. Microbiol.* **57,** 1797–1807
20. DiRuggiero, J., Dunn, D., Maeder, D. L., Holley-Shanks, R., Chatard, J., Horlacher, R. Robb, F. T., Boos, W., and Weiss, R. B. (2000) *Mol. Microbiol.* **38,** 684–693
21. Horlacher, R., Xavier, K. B., Santos, H., DiRuggiero, J., Kossmann, M., and Boos, W. (1998) *J. Bacteriol.* **180,** 680–689
22. Greller, G., Horlacher, R., DiRuggiero, J., and Boos, W. (1999) *J. Biol. Chem.* **274,** 20259–20264
23. Qu, Q., Lee, S.-J., and Boos, W. (2004) *J. Biol. Chem.* **279,** 47890–47897
24. Qu, Q., Lee, S.-J., and Boos, W. (2004) *Extremophiles* **8,** 301–308
25. Koning, S. M., Konings, W. N., and Driessen, A. J. M. (2002) *Archaea* **1,** 19–25
26. Evdokimov, A. G., Anderson, D.E., Routzahn, K. M., and Waugh, D. S. (2001) *J. Mol. Biol.* **305,** 891–904
27. Gill, S., and Hippel, P. (1989) *Anal. Biochem.* **182,** 319–326
28. Kabsch, W. (1993) *J. Appl. Crystallogr.* **26,** 795–800
29. Terwilliger, T. C., and J. Berendzen. (1999) *Acta Crystallogr. D* **55,** 849–861
30. Terwilliger, T. C. (2002) *Acta Crystallogr. D* **59,** 34–44
31. Collaborative Computational Project (1994) *Acta Crystallogr. D* **50,** 760–763
32. Emsley, P., and Cowtan, K. (2004) *Acta Crystallogr. D* **60,** 2126–2132
33. Murshudov, G. N., Vagin, A. A., and Dodson, E. J. (1997) *Acta Crystallogr. D* **53,** 240–245
34. Murshudov, G. N., Lebedev, A., Vagin, A. A., Wilson, K. S., and Dodson, E. J. (1999) *Acta Crystallogr. D* **55,** 247–255
35. Richarme, G., and Kepes, A. (1983) *Biochim. Biophys. Acta* **742,** 16–24
36. Dippel, R., and Boos, W. (2005) *J. Bacteriol.* **187,** 8322–8331
37. Lewis, M., Chang, G., Horton, N. C., Kercher, M. A., Pace, H. C., Schumacher, M. A., Brennan, R. G., and Lu, P. (1996) *Science* **271,** 1245–1254
38. Hars, U., Horlacher, R., Boos, W., Welte, W., and Diederichs, K. (1998) *Protein Sci.* **7,** 2511–2521
39. Clarke, T. E., Ku, S.-Y., Dougan, D. R., Vogel, H. J., and Tari, L. W. (2000) *Nat. Struct. Biol.* **7,** 287–291
40. Borths, E. L., Locher, K. P., Lee, A. T., and Rees, D. C. (2002) *Proc. Natl. Acad. Sci. U. S. A.* **99,** 16642–16647
41. Quiocho, F. A., and Ledvina, P. S. (1996) *Mol. Microbiol.* **20,** 17–25
42. Holm, L., and Sander, C. (1993) *J. Mol. Biol.* **233,** 123–138
43. Diederichs, K., Karplus, P.A. (1997) *Nat. Struct. Biol.* **4**, 269–275